



Fourier transforms infrared spectra and structure of triformylmethane. A density functional theoretical study

Alireza Nowroozi^a, Sayyed Faramarz Tayyari^{a,*}, Hedayat Rahemi^b

^a Department of Chemistry, Ferdowsi University of Mashhad, P.O. Box 1436, Mashhad 91779-1436, Iran

^b Department of Chemistry, Urmia university, Urmia, Iran

Received 4 September 2002; received in revised form 6 November 2002; accepted 6 November 2002

Abstract

Molecular structure and vibrational frequencies of triformylmethane have been investigated by means of density functional theory (DFT) calculations. The geometrical parameters and vibrational frequencies obtained in the B3LYP, B3PW91, BLYP, BPW91, G96LYP and G96PW91 levels of DFT and compared with the corresponding parameters of malonaldehyde (MA). Fourier transform infrared spectra of triformylmethane and its deuterated analogue were clearly assigned. Theoretical calculations show that the hydrogen bond strength of triformylmethane is stronger than that of MA, which is in agreement with spectroscopic results.

© 2002 Elsevier Science B.V. All rights reserved.

Keywords: Triformylmethane; Intramolecular hydrogen bond; FT-IR spectra; Density functional theory; β -Tricarbonyl

1. Introduction

Hydrogen bonding is one of the most important concepts in chemistry, it is crucial to understand many different interactions both in the gas phase and in condensed media. A particular subject is represented by intramolecular hydrogen bonds (IHB), where two functional groups of the same molecule interact, resulting in a ring like structure. β -Dicarbonyl compounds, as interesting examples, display a tautomeric equilibrium between the keto and the enol forms. The chelated *cis* enol forms

are stabilized by a strong IHB [1–4]. This form is usually predominant in the gas phase and in solution with low dielectric constant, such as CCl_4 , CHCl_3 , CH_2Cl_2 and cyclohexane [5,6]. The simplest members of this class of compounds are malonaldehyde (MA) and acetylacetone (AA), well known both by experimental and theoretical studies to adopt an asymmetrical structure in their most stable conformation [7–13].

The vibrational spectra of these compounds have been the subject of a numerous investigations, which supports the existence of a strong IHB of chelating nature in the enol form of β -dicarbonyl [14–21]. This hydrogen bond formation leads to an enhancement of the resonance conjugation of the π -electrons, which causes a marked tendency for equalization of the bond orders of the

* Corresponding author. Tel.: +98-511-878-0216; fax: +98-511-843-8032.

E-mail address: tayyari@ferdowsi.um.ac.ir (S.F. Tayyari).

valence bonds in the resulting six member chelated ring. Therefore, it seems that any parameter that affects the electron density of the chelated ring will change the hydrogen bond strength. It is well known that substitution in α -position drastically changes the hydrogen bond strength and the equilibrium between the enol and keto tautomers [22]. Several experimental data suggest that strength of such a bridge enhances when an electron-withdrawing or bulky groups, replaces the H atom in the α -position [23–27]. Formyl group have the various substitution effects, such as mesomeric, electron withdrawing and steric effects, therefore, potentially is interesting.

Triformylmethane (TFM) is unique among α -substituted MA derivatives so far investigated [28,29], since TFM plays a similar role in the chemistry of β -tricarboxyl, as does MA in the chemistry of β -dicarbonyls. The keto–enol equilibrium of TFM is shown in Fig. 1. In this equilibrium, there are two *cis* enol forms, which are both involved, in IHB. The only difference between these two conformers is due to the orientation of $C_3=C_4$ and $C_9=O_{10}$ double bonds with respect to one another.

It has been shown that TFM completely exists in the enol form, even in the $CHCl_3$ solution [28], whereas AA exhibit 17% keto form [29]. Attempts to obtain an X-ray crystal structure have so far, failed [30]; however, a microwave study for gas phase structure exists [31]. This author reported the *cis* form (2), as the most stable form, based on the simple bond moment calculation. Theoretical study of TFM [25] shows that the *trans* form (1) is more stable than the *cis* form (2), in contrast with the conclusion from the microwave study [31]. Except for these few studies, as far as we know, no

further experimental and theoretical data about the structure of TFM has been reported.

The aims of the present paper are: (1) to predict the structure, *cis* or *trans*, and vibrational spectra (harmonic wave numbers and relative intensities for Raman and IR spectra) of triformylmethane by means of density functional theory (DFT) levels, in solvent such as CCl_4 and $CHCl_3$. (2) Although the TFM is the simplest β -tricarboxyl, no spectroscopic data has been reported for this compound yet. Therefore, in this report we will attempt to present a clear vibrational assignment of TFM by considering the infrared spectrum of its deuterated analogue and theoretical calculations. (3) Comparison of TFM and MA geometrical parameters gives a clear understanding of substitution effects of formyl group on structure, hydrogen bonding and vibrational spectra of the system. (4) We will show that the DFT calculation can accurately predict the vibrational frequencies of TFM.

2. Experimental

Triformylmethane was prepared according to the method of Arnold and žemlička by react the bromoacetic acid with a mixture of phosphorous oxychloride and dimethyl formamide. Crude product was purified by sublimation under reduced pressure. Melting point (m.p.) 105.2 °C; literature 104–106 °C [32]. 1H -NMR: δ 9.03 (s, 2H, one CH=O and one =CH–OH both groups involved in the IHBing); δ 9.47 (s, 1H, free CH=O); δ 13.71 (br, s, 1H, enolic proton). Solution of DTFM in CCl_4 and $CHCl_3$ was prepared by readily exchange with D_2O , then separated the

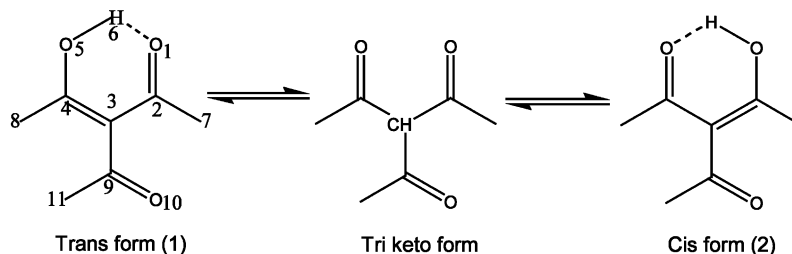


Fig. 1. Keto–enol tautomerism in TFM.

organic layer and dried over the anhydrous Na_2SO_4 . Solutions of TFM and DTFM in solvent were made with a constant mole ratio: 1 mol of solute to 20 mol of solvent.

The FT-IR spectra were taken on a Shimadzu 4300 spectrometer. The $^1\text{H-NMR}$ spectra were obtained on a FT- $^1\text{H-NMR}$, Bruker Aspect 3000 spectrometer at 100 MHz frequencies using 2 mol.% solutions in CDCl_3 at 22 °C. Any attempt for taking the FT-Raman spectrum in the solution failed.

3. Method of analysis

In the present study, the molecular equilibrium geometry, harmonic force field, and vibrational transitions of TFM were computed with the GAUSSIAN 98 software system [33] by using a selection of modern density functionals. The B [34], B3 [35] and G96 [36] exchange functionals were combined with the PW91 [37] and LYP [38] correlation functionals, resulting in the six different functionals BPW91, BLYP, B3PW91, B3LYP, G96PW91 and G96LYP. A series of calculations on TFM were performed with the medium size 6-31G** basis set (125 basis function and 224 primitive Gaussians). Superior results were obtained with B3LYP, combining the hybrid gradient—corrected correlation functionals proposed by Becke with the gradient—corrected correlation functional of Lee, Yang, and Parr. Application of B3LYP density functional was repeated with the largest basis set 6-311++G**, which is a triple-zeta split valence set augmented with diffuse and polarization functions on all atoms (182 basis function, 288 primitive Gaussians).

4. Results and discussions

4.1. Molecular geometry

Tautomerism equilibrium given in Fig. 1 shows that there are two possible enol forms capable to form IHBs, *trans* form (1) and *cis* form (2). The difference between these two forms is the position

of $\text{C}_9=\text{O}_{10}$ and $\text{C}_3=\text{C}_4$ double bonds, with respect to one another. These two forms interchange either by rotation of the α -substituted formyl group about C_3-C_9 bond or proton tunneling between two oxygen atoms. Turner by microwave spectroscopy study suggested that the *cis* form (2) is more stable than *trans* form (1), whereas the result of ab initio calculation emphasizes on the *trans* form. For removing this duality, we carried out extensive theoretical calculations at B3LYP, B3PW91, BLYP, BPW91, G96LYP and G96PW91 levels with 6-31G** basis set. Furthermore, calculations of energy gap (ΔE) between these two conformers in B3LYP level at various basis sets can be used to elucidate the effect of basis set size. The results of these calculations are given in Table 1.

The result of our calculations show that at all of the DFT levels, with 6-31G** basis set, the *trans* form is more stable than the *cis* form and the values of ΔE are lie in the range of 0.88–1.24 kJ mol^{-1} . The maximum and minimum energy gap (ΔE) corresponds to the B3LYP and G96PW91 levels of theory, respectively. As it is evident from

Table 1
Comparison of energy gap (ΔE) between the *cis* and *trans* conformers

Calculation level	<i>trans</i> form	<i>cis</i> form	ΔE (kJ mol^{-1})
BLYP/6-31G**	−380.397512	−380.397142	0.970
BPW91/6-31G**	−380.454843	−380.454504	0.886
G96LYP/6-31G**	−380.379933	−380.379596	0.883
G96PW91/6-31G**	−380.437891	−380.437555	0.880
B3LYP/6-31G**	−380.484908	−380.484433	1.243
B3PW91/6-31G**	−380.336175	−380.335812	0.962
B3LYP/STO-3G	−375.422982	−375.422988	0.000
B3LYP/3-21G	−378.372350	−378.372182	0.440
B3LYP/4-31G	−379.962870	−379.962553	0.830
B3LYP/6-31G*	−380.474732	−380.474244	1.278
B3LYP/6-31G**	−380.484908	−380.484433	1.243
B3LYP/6-311G*	−380.575361	−380.574700	1.733
B3LYP/6-311G**	−380.587084	−380.586437	1.695
B3LYP/6-311+	−380.597737	−380.596927	2.124
G**			
B3LYP/6-311++	−380.597891	−380.597087	2.106
G**			

Absolute energies in Hartree.

Table 2
Geometrical parameters of *trans* form of TFM and MA at various DFT levels with 6-31G** basis set^a

Structural parameters	TFM							MA							Experimental ^c
	B3LYP ^b	B3LYP	BLYP	B3PW91	BPW91	G96LYP	G96PW91	B3LYP ^a	B3LYP	BLYP	B3PW91	BPW91	G96LYP	G96PW91	
R_{1-2}	1.234	1.242	1.260	1.241	1.260	1.260	1.261	1.238	1.245	1.265	1.246	1.265	1.265	1.266	1.234
R_{2-3}	1.454	1.451	1.454	1.445	1.446	1.452	1.443	1.438	1.437	1.440	1.431	1.432	1.437	1.429	1.454
R_{3-4}	1.374	1.378	1.393	1.379	1.394	1.394	1.395	1.364	1.368	1.383	1.369	1.384	1.383	1.385	1.348
R_{4-5}	1.308	1.308	1.319	1.301	1.309	1.315	1.305	1.319	1.319	1.330	1.312	1.319	1.327	1.315	1.320
R_{5-6}	1.004	1.015	1.043	1.022	1.060	1.048	1.068	0.997	1.007	1.034	1.014	1.049	1.038	1.057	0.969
R_{1-6}	1.666	1.615	1.563	1.562	1.487	1.534	1.453	1.700	1.641	1.592	1.586	1.512	1.566	1.478	1.680
R_{1-5}	2.563	2.535	2.528	2.502	2.481	2.508	2.459	2.587	2.554	2.546	2.517	2.494	2.528	2.472	2.553
R_{2-7}	1.098	1.100	1.107	1.100	1.106	1.106	1.105	1.103	1.105	1.112	1.104	1.110	1.111	1.109	1.089
R_{4-8}	1.088	1.091	1.098	1.092	1.099	1.098	1.099	1.086	1.089	1.096	1.090	1.097	1.096	1.097	1.091
R_{3-9}	1.464	1.463	1.473	1.460	1.468	1.472	1.467	1.081	1.083	1.090	1.082	1.089	1.089	1.088	1.094
R_{9-10}	1.213	1.219	1.232	1.217	1.229	1.231	1.228								
R_{9-11}	1.111	1.114	1.123	1.114	1.123	1.123	1.122								
θ_{1-2-3}	122.4	122.5	122.5	122.4	122.3	122.4	122.2	123.3	123.4	123.2	123.2	122.9	123.1	122.7	124.5
θ_{2-3-4}	118.9	118.3	117.9	117.8	117.3	117.6	116.9	119.7	118.9	118.6	118.3	117.8	118.4	117.5	119.4
θ_{3-4-5}	124.4	123.9	123.4	123.5	122.9	123.2	122.6	124.2	123.9	123.4	123.6	122.9	123.2	122.7	123.0
θ_{4-5-6}	106.6	105.6	104.3	105.0	103.6	104.1	103.3	106.6	105.4	104.2	104.8	103.4	104.0	103.1	106.3
θ_{5-6-1}	146.4	148.8	151.2	150.4	153.4	152.0	154.3	145.9	148.5	150.9	150.1	153.2	151.7	154.1	147.6
θ_{1-2-7}	120.5	120.4	120.1	120.3	119.9	120.0	119.7	119.1	118.9	118.7	118.8	118.4	118.6	118.3	122.3
θ_{5-4-8}	113.9	114.3	114.5	114.6	115.1	114.7	115.3	113.3	113.6	113.8	113.9	114.3	114.0	114.6	113.2
θ_{2-3-9}	121.3	121.0	121.1	121.1	121.3	121.3	121.6	120.3	120.7	120.8	121.0	121.3	121.0	121.4	123
θ_{3-9-10}	124.7	124.4	124.4	124.3	124.4	124.6	124.5								
θ_{3-9-11}	114.7	114.7	114.5	114.8	114.5	114.5	114.5								
Q_1	0.074	0.066	0.059	0.06	0.049	0.055	0.044	0.081	0.074	0.065	0.066	0.054	0.062	0.049	0.086
Q_2	0.08	0.073	0.061	0.066	0.052	0.058	0.048	0.074	0.069	0.057	0.062	0.048	0.054	0.044	0.106
Q	0.154	0.139	0.120	0.126	0.101	0.113	0.092	0.155	0.143	0.122	0.128	0.102	0.116	0.093	0.192
E_{HB}	56.0	64.1	66.2	66.2	69.4	66.5	70.0	54.0	62.7	65.0	64.9	68.4	64.9	68.6	

^a R , bond length (Å); θ , bond angle (°); E_{HB} , hydrogen bond energy (kJ mol⁻¹).

^b Calculated at B3LYP/6-311++G** level.

^c Data from [40].

Table 3
Calculated (*trans* form) and experimental rotational constant

Level of calculation	<i>A</i>	<i>B</i>	<i>C</i>	Relative error (%)
B3LYP/6-311++G**	4.932	2.025	1.436	0.34
B3LYP/6-31G**	4.984	2.020	1.438	0.57
B3PW91/6-31G**	5.066	2.025	1.447	1.11
BLYP/6-31G**	4.971	1.982	1.417	1.59
BPW91/6-31G**	5.080	1.990	1.430	1.89
G96LYP/6-31G**	5.014	1.982	1.420	1.81
G96PW91/6-31G**	5.130	1.990	1.433	2.16
Experimental ^a	4.944	2.034	1.441	–

Rotational constant (GHz).

^a Data from [31].

The electron withdrawing character of the formyl group lowers the electron charge density on the oxygen atoms, which in turn causes the enolated proton to be more acidic and increases the hydrogen bond strength. The effect of the formyl group on the π -delocalization in the chelated ring could also be explained in terms of the Gilli's symmetry coordinates q_1 , q_2 and Q [41] (see Table 2). By comparing of these coordinates for TFM and MA, one can deduce that there is more bond equalization, or π -delocalization, in formyl substituted MA than in MA itself.

5. Vibrational analysis

The fundamental vibrational frequencies for TFM obtained at different DFT levels with 6-31G** basis set, are compared with the experimental values by means of regression analysis. The superior quality result is produced from the B3LYP level with the more expensive 6-311++G** basis set (see Table 4). In the regression analysis a set of 20 vibrational bands was selected, corresponding to fundamentals numbers: ν_1 – ν_{17} , ν_{20} and ν_{21} . The regression parameters, least squares scaling factor (α), *R* square and standard deviation (S.D.), are listed in Table 5. As it is obvious in this table, the best results are obtained with B3LYP, resulting in S.D. = 28.4 and 9.46 cm^{-1} for B3LYP/6-31G** and B3LYP/6-311++G**, respectively. It is noteworthy to point out

that addition of polarized and diffused functions on the basis set, in the DFT, leads to better correlation with the experimental frequencies.

The infrared spectrum of TFM and its deuterated analogues (DTFM) in CCl_4 solution is given in Fig. 2. The calculated frequencies, IR intensity at B3LYP/6-311++G** level along with the experimental results and their assignments for TFM and its deuterated analogue are given in Tables 6 and 7. The corresponding normal modes of the chelated ring are shown in Fig. 3. The calculated frequencies and isotopic shifts are slightly higher than the observed values for the majority of the normal modes. Two factors may be responsible for the discrepancy between the experimental and computed spectra of TFM. The first is caused by the environment; the second reason for this discrepancy is the fact that the experimental value is an anharmonic frequency while the calculated value is a harmonic frequency.

5.1. Band assignment

Each equilibrium configuration of TFM has C_s symmetry, which leads to 19 in plane (A') and eight out of plane (A'') vibrational normal modes, which all of them are IR active. The band assignments presented here obey the following criteria: (a) the observed band frequencies and intensity changes in the infrared spectrum [13,16] of the deuterated analogue confirmed by establishing one

Table 4
Comparison of experimental and theoretical vibrational frequencies (cm^{-1})

	B3LYP ^a	B3LYP ^b	B3PW91 ^b	BLYP ^b	BPW91 ^b	G96LYP ^b	G96PW91 ^b	Experimental
<i>A'</i>								
ν_1	3157	3164	3167	3070	3078	3073	3078	3062
ν_2	3072	3058	3071	2973	3000	2982	3011	2820
ν_3	3034	2927	2898	2775	2795	2778	2799	2792
ν_4	2876	2886	2806	2551	2340	2482	2244	2743
ν_5	1761	1792	1807	1705	1727	1710	1733	1700
ν_6	1702	1725	1735	1635	1649	1638	1653	1658
ν_7	1625	1658	1672	1614	1638	1622	1647	1595
ν_8	1445	1462	1461	1415	1419	1417	1423	1411
ν_9	1435	1451	1458	1388	1394	1389	1396	1401
ν_{10}	1391	1408	1409	1351	1342	1348	1344	1329
ν_{11}	1366	1374	1374	1327	1322	1327	1309	1345
ν_{12}	1299	1317	1325	1276	1288	1283	1288	1264
ν_{13}	1234	1249	1255	1203	1210	1204	1206	1212
ν_{14}	939	956	965	926	937	929	939	930
ν_{15}	736	742	743	719	721	720	721	
ν_{16}	527	538	541	531	538	534	542	520
ν_{17}	499	502	504	485	489	485	490	486
ν_{18}	281	283	285	286	295	290	302	
ν_{19}	212	212	206	206	198	202	194	
<i>A''</i>								
ν_{20}	1049	1069	1101	1079	1141	1103	1172	1020
ν_{21}	1034	1046	1048	1005	1006	1007	1009	1004
ν_{22}	1000	1018	1025	983	987	986	990	970
ν_{23}	929	951	957	917	926	922	931	909
ν_{24}	390	400	397	391	387	391	387	
ν_{25}	324	346	348	344	349	346	352	
ν_{26}	242	259	261	257	260	258	260	
ν_{27}	131	142	143	137	137	137	137	

^a Calculated by 6-311++G**.

^b Calculated by 6-31G**.

to one correlation between observed and theoretically calculated frequencies. (b) Comparison in some cases with reported vibrational assignment of characteristic molecular groups and bonds found in different molecules. (c) The visual 3D computerized representation of the normal modes.

5.2. 3100–1800 cm^{-1}

In this region the C–H and O–H/O–D stretching band frequencies are expected to be observed. $\nu_{\text{O–H}}$ is the most important mode in vibrational spectra of β -dicarbonyl compounds, which is

Table 5
Regression analysis of fundamental wave numbers with theoretical corresponds

Regression parameters	B3LYP ^a	B3LYP ^b	B3PW91 ^b	BLYP ^b	BPW91 ^b	G96LYP ^b	G96PW91 ^b
R square	0.99986	0.99880	0.99788	0.99420	0.98270	0.99160	0.97410
S.D.	9.65	28.43	37.90	61.30	108.37	75.32	132.40
Regression coefficient	0.9754	0.9658	0.9626	1.0007	1.0040	1.0025	1.0005

^a Calculated by 6-311++G**.

^b Calculated by 6-31G**.

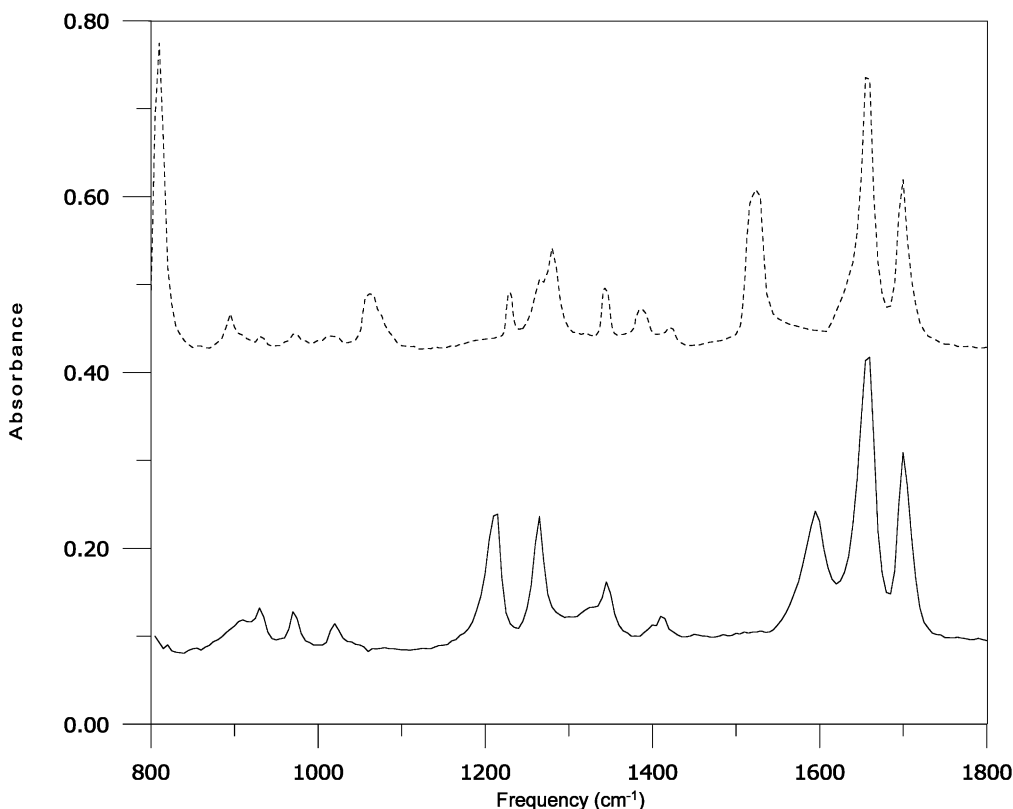


Fig. 2. Infrared spectrum of TFM (—) and DTFM (----).

related to the IHB strength. Determination of the precise position of O–H stretching of the enol form of β -dicarbonyls is very difficult because it appears as a very broad band [12–16] and overlaps by the C–H stretching, overtones and combination bands. Tayyari et al. [13,16] carried out an extensive spectroscopic study of hydrogen bonding in the enol form of β -dicarbonyl compounds and proposed a dependence of O–H stretching frequency on the O...O distance. Theoretical calculations predict that the O...O distance in TFM is shorter than MA (about 0.025 Å). Therefore, we expect that the O–H stretching frequency in TFM to lie in below 2850 cm^{-1} , which is observed in MA. A weak and broad band in this region was observed, but location the center of this band is difficult. Since the $\nu\text{O–H}/\nu\text{O–D}$ ratio in TFM is 1.35 and O–D stretching observed at 2089 cm^{-1} we might predict the center of O–H stretching

band at about 2820 cm^{-1} . This value is in agreement with the theoretical results. Lower frequency of O–H/O–D stretching modes in TFM/DTFM in comparison with the corresponding value for MA/D2MA also supports the idea that the hydrogen bond in TFM is stronger than that of MA. The $\nu\text{O–H}$ and $\nu\text{O–D}$ bands in MA appear at 2856 and 2140 cm^{-1} , respectively [12].

The infrared spectrum of TFM shows three weak bands at 3062, 2792, and 2743 cm^{-1} . These bands readily are correlated with theoretical bands at 3156, 3036 and 2876 cm^{-1} , respectively. As other β -dicarbonyls in their enol form, the vinyl $\text{C}_4\text{–H}_8$ stretching frequency should appear at higher frequency than other C–H stretching modes [12]. Theoretical calculations predict that this band is mainly due to $\nu\text{C}_4\text{–H}_8$, which is slightly coupled to $\nu\text{O–H}$ and upon deuteration a few wave number shifts toward lower frequencies

Table 6
Fundamental band assignment of TFM (frequencies are in cm^{-1} and intensities are relative)

	Theoretical frequency		Experimental frequency (IR)		Assignment
	B3LYP/6-311++G**	R.I. ^a	TFM(CCl ₄)	TFM(CHCl ₃)	
<i>A'</i>					
ν_1	3156(1) ^b	40	3062	*	$\nu\text{C}_4\text{H}_8 + \nu\text{OH}$
ν_2	3077(63)	58	2820(w,vbr)	*	$\nu\text{OH} + \nu\text{C}_4\text{H}_8 + \nu\text{C}_2\text{H}_7$
ν_3	3036(12)	49	2792	2787	$\nu\text{C}_2\text{H}_7$
ν_4	2876(23)	100	2743	2739	$\nu\text{C}_9\text{H}_{11}$
ν_5	1760(54)	58	1700(77)	1699(67)	$\nu\text{C}_9\text{O}_{10} + \delta\text{C}_9\text{H}_{11}$
ν_6	1702(100)	10	1658(100)	1657(100)	$\nu\text{C}_1\text{O}_2 + \nu\text{C}_3\text{C}_4 + \delta\text{C}_2\text{H}_7 + \delta\text{C}_4\text{H}_8$
ν_7	1625(54)	31	1595(50)	1597(55)	$\nu\text{C}_3\text{C}_4 + \nu\text{C}_2\text{O}_1 + \delta\text{OH} + \delta\text{C}_4\text{H}_8$
ν_8	1446(6)	4	1411(12)	1415(11)	$\delta\text{C}_9\text{H}_{11} + \delta\text{C}_4\text{H}_8 + \delta\text{OH} + \nu\text{C}_2\text{C}_3$
ν_9	1436(4)	7.4	1401(sh)	1405(sh)	$\nu\text{C}_4\text{O}_5 + \nu\text{C}_2\text{O}_1 + \delta\text{C}_2\text{H}_7 + \delta\text{C}_4\text{H}_8 + \delta\text{OH}$
ν_{10}	1391(11)	7.4	1329(15)	1336(12)	$\delta\text{OH} + \nu\text{C}_3\text{C}_4 + \delta\text{C}_2\text{H}_7 + \delta\text{C}_9\text{H}_{11}$
ν_{11}	1365(21)	7.5	1345(32)	1349(32)	$\delta\text{C}_2\text{H}_7 + \delta\text{C}_9\text{H}_{11} + \delta\text{C}_4\text{H}_8$
ν_{12}	1299(41)	0.74	1264(60)	1268(48)	$\nu\text{C}_4\text{O}_5 + \delta\text{C}_4\text{H}_8 + \delta\text{OH}$
ν_{13}	1233(31)	13.3	1212(65)	*	$\nu\text{C}_3\text{C}_9 + \delta\text{C}_2\text{H}_7 + \delta\text{OH} + \delta\text{C}_4\text{H}_8$
ν_{14}	938(7)	13.3	930(19)	935(22)	$\delta\text{C}_2\text{C}_3\text{C}_4 + \delta\text{C}_2\text{H}_7 + \delta\text{C}_4\text{H}_8 + \delta\text{OH}$
ν_{15}	736(9)	0.2	*	*	$\Delta + \delta\text{C}_2\text{H}_7$
ν_{16}	527(4)	0.4	520(10)	521(14)	$\Delta + \delta\text{C}-\text{CHO}$
ν_{17}	499(0.3)	7.4	486(6)	488(6)	$\Delta + \delta\text{C}-\text{CHO}$
ν_{18}	278(1.5)	0.74	n.m.	n.m.	$\nu(\text{O}\cdots\text{O})$
ν_{19}	213(3)	~0	n.m.	n.m.	$\Delta + \delta\text{C}-\text{CHO}$
<i>A''</i>					
ν_{20}	1049(10)	0.74	1020(10)	1017(11)	$\gamma\text{C}_2\text{H}_7 + \gamma\text{C}_9\text{H}_{11} + \gamma\text{C}_4\text{H}_8$
ν_{21}	1035(3)	0.74	1005(5)	1008(5)	$\gamma\text{C}_2\text{H}_7 + \gamma\text{C}_9\text{H}_{11} + \gamma\text{OH}$
ν_{22}	1000(7)	1.5	970(15)	974(13)	$\gamma\text{C}_9\text{H}_{11} + \gamma\text{C}_2\text{H}_7 + \gamma\text{C}_4\text{H}_8 + \gamma\text{OH}$
ν_{23}	928(7)	1.5	909(sh)	911(sh)	$\gamma\text{OH} + \gamma\text{C}_9\text{H}_{11} + \gamma\text{C}_4\text{H}_8$
ν_{24}	391(0.25)	0.35	n.m.	n.m.	$\Gamma + \gamma\text{C}-\text{CHO}$
ν_{25}	326(2)	~0	n.m.	n.m.	$\Gamma + \gamma\text{C}-\text{CHO}$
ν_{26}	244(0.2)	0.2	n.m.	n.m.	$\Gamma + \gamma\text{C}-\text{CHO}$
ν_{27}	131(3)	1	n.m.	n.m.	$\Gamma + \gamma\text{C}-\text{CHO}$

IR, infrared; ν , stretching; δ , in plane bending; γ , out of plane bending; Δ , in plane ring deformation; Γ , out of plane ring deformation; v, very; sh, shoulder; n.m., not measured; *, solvent overlapped, relative intensities are given in parentheses.

^a Relative intensity in Raman.

^b Relative intensity in IR.

(about 7 cm^{-1}). It is noteworthy that the observed $\nu\text{C}_2-\text{H}_7$ is much lower than that predicted by the calculations. The aldehyde C–H stretching usually shows two bands in the $2900-2700\text{ cm}^{-1}$ range with one near 2720 cm^{-1} [44]. This phenomenon has been attributed to an interaction of the C–H stretch fundamental with the overtone of the C–H bending vibration at about 1400 cm^{-1} . Therefore, discrepancy between the calculated and observed $\nu\text{C}_2-\text{H}_7$ could be attributed to the neglecting this interaction by the ab initio calculations. Furthermore frequency measurement has been done in the

solution and calculation assumes the molecule in the gas phase. By considering the theoretical calculations, we assign the bands at about 2790 and 2740 cm^{-1} in the infrared spectra of TFM and its deuterated analogue to $\nu\text{C}_2-\text{H}_7$ and $\nu\text{C}_9-\text{H}_{11}$, respectively.

5.3. $1700-1000\text{ cm}^{-1}$

Beside the C=O stretching of free carbonyl group and C–H in-plane bending modes, five bands are expected to be observed in this region,

Table 7
Fundamental band assignment of DTFM (frequencies are in cm^{-1} and intensities are relative)

	Theoretical frequency	Experimental frequency (IR)			Assignment
		B3LYP/6-311++G**	R.I. ^a	DTFM(CCl_4)	
<i>A'</i>					
ν_1	3151(1.6) ^b	64	3055	*	$\nu\text{C}_4\text{H}_8$
ν_2	3035(5)	60	2790	2788	$\nu\text{C}_2\text{H}_7$
ν_3	2878(23)	100	2740	2736	$\nu\text{C}_9\text{H}_{11}$
ν_4	2260(47)	9	2089(6)	2085(7)	νOD
ν_5	1760(55)	58	1700(65)	1698(61)	$\nu\text{C}_9\text{O}_{10} + \delta\text{C}_9\text{H}_{11}$
ν_6	1702(100)	9.5	1657(100)	1655(100)	$\nu\text{C}_1\text{O}_2 + \nu\text{C}_3\text{C}_4 + \delta\text{C}_2\text{H}_7 + \delta\text{C}_4\text{H}_8$
ν_7	1558(54)	4	1523(62)	1526(55)	$\nu\text{C}_3\text{C}_4 + \nu\text{C}_1\text{O}_2 + \delta\text{OD} + \delta\text{C}_4\text{H}_8$
ν_8	1445(8)	1.5	1408(7)	1410(7)	$\nu\text{C}_2\text{C}_3 + \delta\text{C}_9\text{H}_{11} + \delta\text{C}_4\text{H}_8$
ν_9	1420(7)	5.2	1388(14)	1391(14)	$\delta\text{C}_2\text{H}_7 + \delta\text{C}_9\text{H}_{11} + \nu\text{C}_2\text{C}_3$
ν_{10}	1370(20)	5.4	1345(30)	1349(33)	$\delta\text{C}_2\text{H}_7 + \delta\text{C}_9\text{H}_{11} + \delta\text{C}_4\text{H}_8$
ν_{11}	1325(38)	1.2	1280(45)	1283(49)	$\nu\text{C}_4\text{O}_5 + \delta\text{OD} + \delta\text{C}_4\text{H}_8$
ν_{12}	1257(4)	9.3	1230(19)	*	$\nu\text{C}_3\text{C}_9 + \delta\text{C}_9\text{H}_{11} + \delta\text{C}_2\text{H}_7 + \delta\text{OD}$
ν_{13}	1100(32)	5.2	1061(27)	1065(28)	$\delta\text{OD} + \delta\text{C}_4\text{H}_8 + \nu\text{C}_2\text{C}_3 + \delta\text{C}_2\text{H}_7$
ν_{14}	910(9)	12	895(15)	895(17)	$\delta\text{C}_2\text{C}_3\text{C}_4 + \delta\text{C}_2\text{H}_7 + \delta\text{OD} + \delta\text{C}_4\text{H}_8$
ν_{15}	730(8)	2	*	*	$\Delta + \delta\text{CCHO}$
ν_{16}	523(4)	2.3	516(13)	517(11)	$\Delta + \delta\text{CCHO}$
ν_{17}	489(0.003)	7.3	480(6)	482(6)	$\Delta + \delta\text{C-CHO}$
ν_{18}	270(1.5)	0.5	n.m.	n.m.	$\nu(\text{O}\cdots\text{O})$
ν_{19}	213(3)	0.45	n.m.	n.m.	$\Delta + \delta\text{C-CHO}$
<i>A''</i>					
ν_{20}	1044(0.01)	0.73	1015(4)	1017(5)	$\gamma\text{C}_2\text{H}_7 + \gamma\text{C}_9\text{H}_{11} + \gamma\text{C}_4\text{H}_8$
ν_{21}	1025(0.01)	2.2	995(5)	998(4)	$\gamma\text{C}_4\text{H}_8 + \gamma\text{C}_9\text{H}_{11}$
ν_{22}	971(1)	1.2	931(5)	934(5)	$\gamma\text{C}_2\text{H}_7 + \gamma\text{C}_9\text{H}_{11} + \gamma\text{C}_4\text{H}_8$
ν_{23}	731(16)	0.25	*	*	$\gamma\text{OD} + \gamma\text{C}_2\text{H}_7$
ν_{24}	379(0.002)	0.3	n.m.	n.m.	$\Gamma + \gamma\text{C-CHO}$
ν_{25}	326(2)	0.21	n.m.	n.m.	$\Gamma + \gamma\text{C-CHO}$
ν_{26}	244(0.003)	0.86	n.m.	n.m.	$\Gamma + \gamma\text{C-CHO}$
ν_{27}	130(3)	1	n.m.	n.m.	$\Gamma + \gamma\text{C-CHO}$

IR, infrared; ν , stretching; δ , in plane bending; γ , out of plane bending; Δ , in plane ring deformation; Γ , out of plane ring deformation; v, very; sh, shoulder; n.m., not measured; *, solvent overlapped, relative intensities are given in parentheses.

^a Relative intensity in Raman.

^b Relative intensity in IR

in relation to the enol ring modes which are attributed to C=O, C=C, C-O and C-C stretching and the O-H in plane bending modes. The observed frequencies in this region are as follows.

The strong band at 1700 cm^{-1} , which is not affected upon deuteration, clearly assigned to the C=O stretching of the free carbonyl group. According to the calculation results, this band is coupled to $\delta\text{C}_9\text{-H}_{11}$. Aliphatic aldehydes have an intense carbonyl stretching band at about 1725 cm^{-1} [44]. Comparison between the band at 1700 cm^{-1} , in infrared spectrum of TFM, and $\nu\text{C=O}$ in

aliphatic aldehyde shows that the carbonyl frequency is shifted toward lower values. This frequency shift arise from conjugation, without hydrogen bonding, in $\text{O}_{10}=\text{C}_9-\text{C}_3=\text{C}_4-\text{O}_5$ fragment. This result is in excellent agreement with the geometrical parameters that emphasize the π -electron delocalization in $\text{O}_{10}=\text{C}_9-\text{C}_3=\text{C}_4-\text{O}_5$ fragment.

In the C=O and C=C stretching region, with exception of hexafluoro-AA [45], trifluoro-AA [13] and MA [12], only one single band has been observed in the IR spectra of the enol form of β -

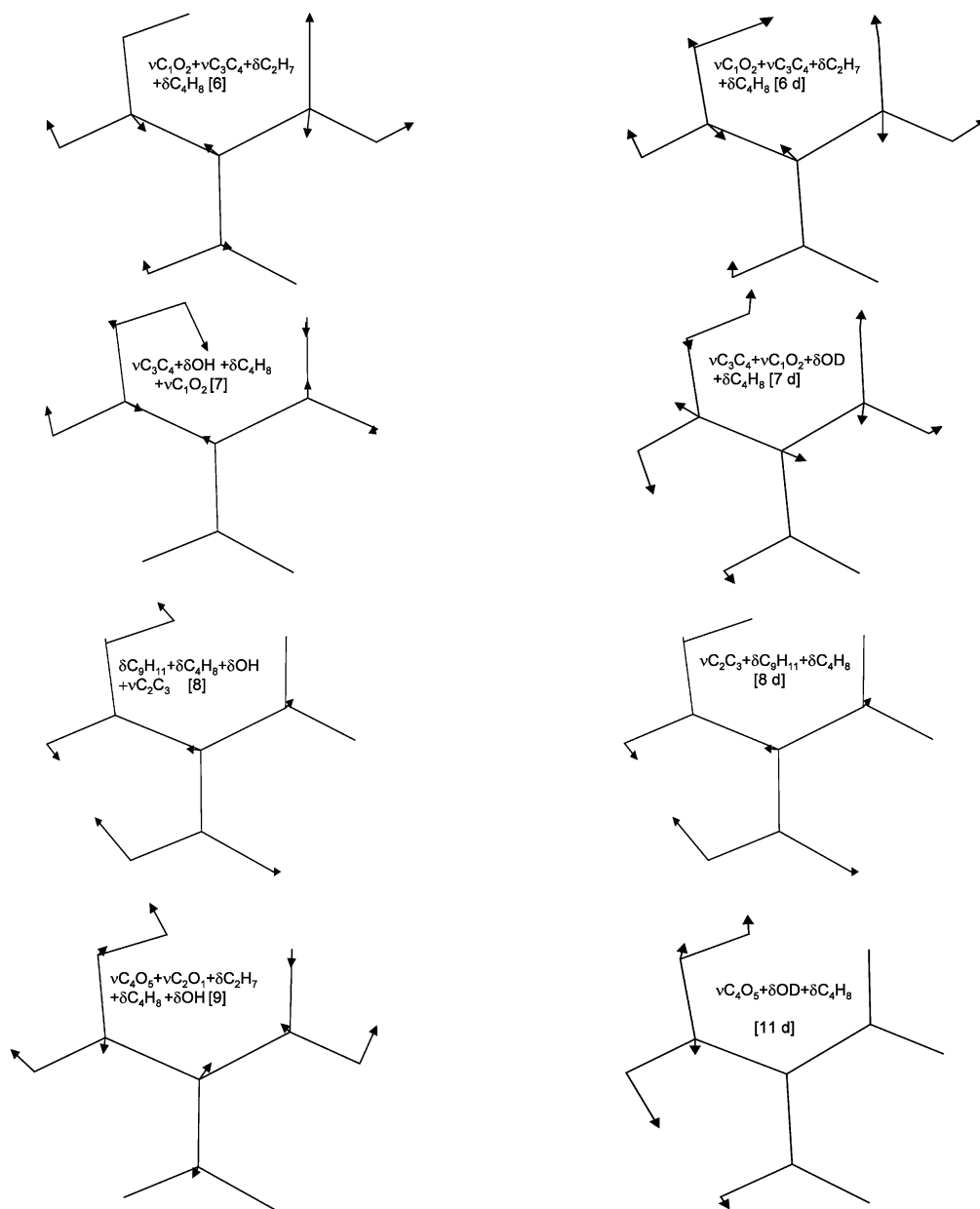


Fig. 3. Selected normal modes of TFM and DTFM.

dicarbonyls [13]. Tayyari et al. by deconvolution of the IR spectra of AA and its deuterated analogue, D6AA [14], and α -cyano-acetylacetone (CNAA) [46] showed that another strong and broad band corresponding to the very strong and relatively broad Raman band, lies under this band

at its lower frequency side. In the case of AA these two bands appear at 1642 and 1624 cm^{-1} in the gas phase and shift considerably toward lower frequencies in the condensed phases [16]. In the infrared spectrum of TFM these two bands are well separated and appear as two strong bands at

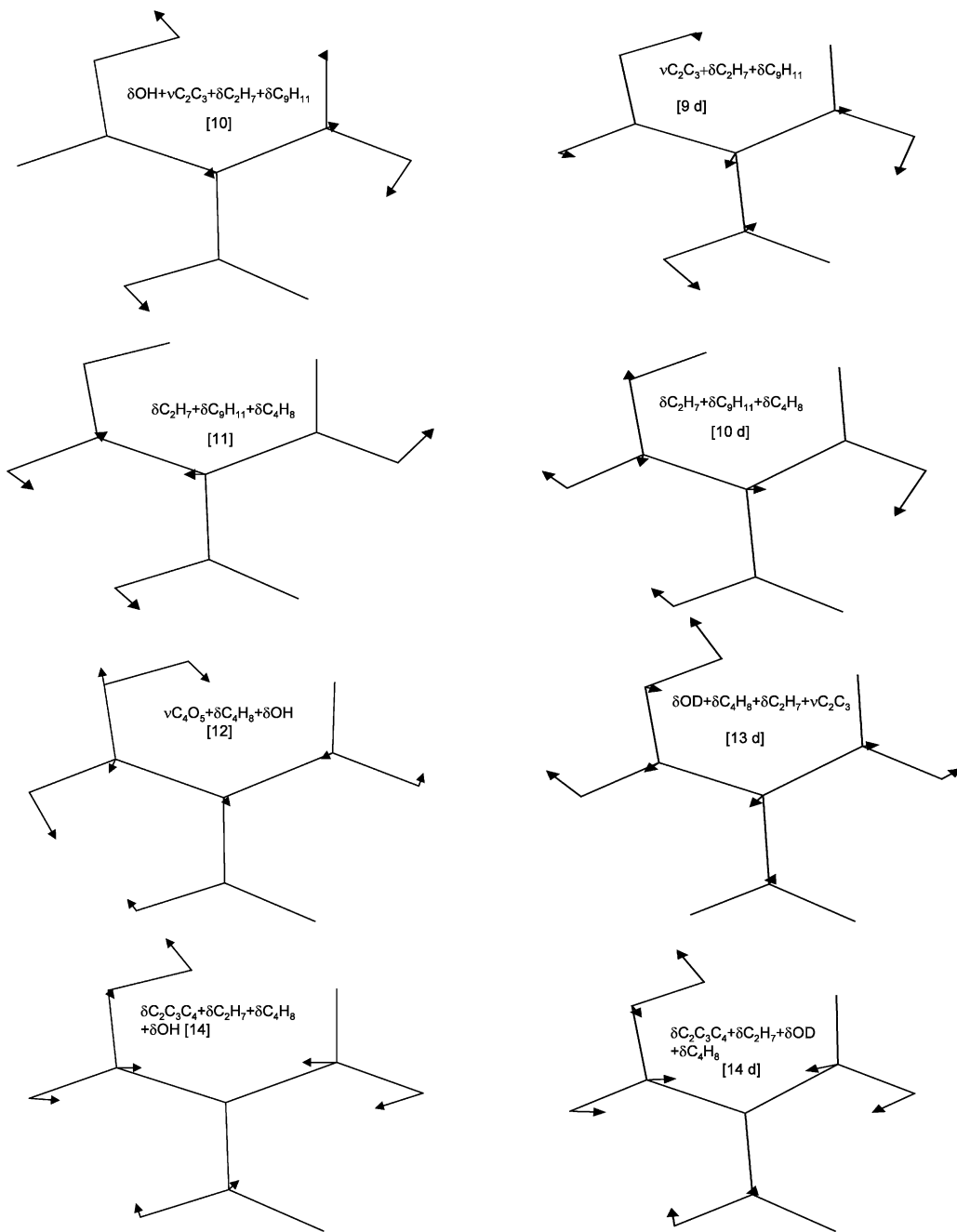


Fig. 3 (Continued)

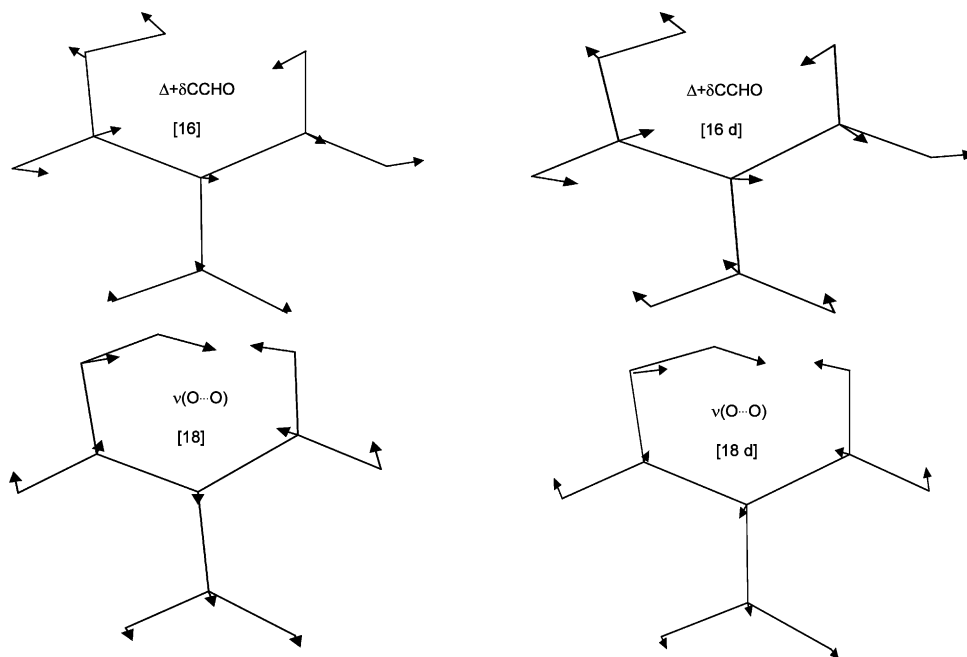


Fig. 3 (Continued)

1658 and 1595 cm^{-1} . Upon deuteration the former is almost unaffected, but the latter shifts about 70 cm^{-1} toward lower frequencies. This frequency shift is in excellent agreement with the result of DFT calculations (see Tables 6 and 7). We assigned the band at 1658 cm^{-1} to the $\text{C}_1=\text{O}_2$ and $\text{C}_3=\text{C}_4$ stretching modes, which are coupled to $\delta\text{C}_2-\text{H}_7$ and $\delta\text{C}_4-\text{H}_8$. Theoretical calculations predict that the infrared band at 1595 cm^{-1} is mainly due to O–H in plane bending and $\text{C}_3=\text{C}_4$ stretching modes, which is coupled to the $\text{C}_1=\text{O}_2$ stretching and C–H₈ in plane bending modes. Since this band has mostly $\text{C}_3=\text{C}_4$ stretching and O–H in plane bending characters, therefore, we believed that there exist strong interactions between these two motions in the chelated ring of the *cis* enol form of β -dicarbonyls. The magnitude of interaction between these two modes, in TFM respect to MA, suggests a much stronger IHB for TFM in agreement with other β -dicarbonyls [46]. The corresponding band in DTFM that appeared in 1523 cm^{-1} is mainly due to the $\text{C}_1=\text{O}_2$ and $\text{C}_3=$

C_4 stretching modes, which is coupled to the O–D and C–H in plane bending modes (see Table 7).

The band at about 1411 cm^{-1} in TFM and 1408 cm^{-1} in its deuterated analogue is mainly due to the $\delta\text{C}_9-\text{H}_{11}$ in plane bending mode and the small frequency shift upon deuteration is correctly predicted by the theoretical calculations. The infrared spectrum of TFM shows a shoulder band at about 1400 cm^{-1} . Theoretical calculations suggest that this band, in TFM, is mainly due to $\nu\text{C}_4-\text{O}_5$ and $\nu\text{C}_2=\text{O}_1$ that couples with $\delta\text{O}-\text{H}$ and $\delta\text{C}-\text{H}$. Upon deuteration, this shoulder disappears and a new band appears at 1280 cm^{-1} . In the TFM the coupling of $\nu\text{C}_2=\text{O}_1$ and $\delta\text{O}-\text{H}$ is completely removed and a large frequency shift, about 120 cm^{-1} , is observed. This shift is in excellent agreement with the experimental results. The band at 1329 cm^{-1} has mixed C–H and O–H in plane bending and C_2-C_3 stretching character. Upon deuteration, this band shift toward higher frequencies and appear at about 1388 cm^{-1} . According to the calculations we assign this

band, in DTFM, to the $\nu\text{C}_2\text{-C}_3$, which couples with $\text{C}_2\text{-H}_7$ and $\text{C}_9\text{-H}_{11}$ in plane bending modes.

The band at about 1265 cm^{-1} has O–H and C–H in plane bending and $\text{C}_4\text{-O}_5$ stretching character. Deuteration causes a large frequency shift on position of this band and it appears at 1061 cm^{-1} in the IR spectrum of DTFM with its intensity decreased. According to the theoretical calculations the band at 1061 cm^{-1} in DTFM is mainly due to $\delta\text{O-D}$, which is coupled to $\delta\text{C}_4\text{-H}_8$ and $\nu\text{C}_2\text{-C}_3$. The IR intensity of this band in DTFM decreases, because the coupling of $\text{C}_4\text{-O}_5$ stretching mode is completely removed.

The strong band at 1212 cm^{-1} shifts about 18 cm^{-1} toward upper frequencies in DTFM, which is also in excellent agreement with the theoretical results. According to the theoretical calculations, the band at 1212 cm^{-1} is due to $\text{C}_3\text{-C}_9$ stretching mode coupled to $\delta\text{O-H}$ and $\delta\text{C-H}$. Upon deuteration this band shifts toward upper frequencies, 1230 cm^{-1} , and its intensity decreases. Both frequency shift and intensity decrease are arises from decoupling of $\delta\text{O-H}$. The increase of π -electron delocalization in the $\text{O}_{10}=\text{C}_9\text{-C}_3=\text{C}_4\text{-O}_5$ fragment, in TFM, shifts the $\text{C}_3\text{-C}_9$ stretching frequency toward higher wave numbers respect to the corresponding band in alkanes [44].

The theoretical calculation suggests that two bands at 1020 and 1005 cm^{-1} have C–H out of plane bending character. However, the latter band has slightly O–H out of plane bending character. In DTFM these two bands shift about 5 and 10 cm^{-1} toward lower frequencies, respectively. These band shifts are in excellent agreement with theoretical predictions. Similarly with TFM, these bands have C–H out of plane bending character.

5.4. Below 1000 cm^{-1}

In this region we expect to observe C–H and O–H out of plane bending and in plane and out of plane ring deformation and $\text{O}\cdots\text{O}$ stretching modes. By considering the theoretical calculations, the IR band at 970 cm^{-1} is assigned mainly to $\gamma\text{C}_9\text{-H}_{11}$, which is slightly coupled to $\gamma\text{C}_4\text{-H}_8$, $\gamma\text{C}_2\text{-H}_7$ and $\gamma\text{O-H}$. Upon deuteration, this band shifts to 931 cm^{-1} and IR intensity considerably

decreases. The reason of this phenomenon is due to the decoupling of $\gamma\text{O-H}$.

It is interesting to note that the frequencies of the in plane ring deformation modes in TFM are considerably higher than the corresponding modes in MA. This could be attributed to the stronger ring in TFM in comparison with MA, which is caused by stronger IHB. The 890 cm^{-1} band in MA appears at 930 cm^{-1} in TFM and the 512 cm^{-1} band in the former splits to two bands in the latter at 486 and 520 cm^{-1} . Coupling of this mode with C–CHO in plane bending causes this splitting. The shifts of these bands upon deuteration are in excellent agreement with the theoretical results.

The shoulder at about 909 cm^{-1} is correlated with the theoretical band at 928 cm^{-1} , which has mostly O–H out of plane bending character. Upon deuteration this band disappears and we expect to observe a new band at about 730 cm^{-1} , but this region of spectra overlapped with the solvent bands. The corresponding band in MA appears at 670 cm^{-1} , which correlate with the medium theoretical band at 684 cm^{-1} [12], which considerably lower than the expected value for TFM. This frequency gap also supports the stronger hydrogen bond in TFM respect that in MA.

MA has only two bands, at 384 and 252 cm^{-1} [12], which belong, to the out of plane ring deformation modes. It seems that the 384 cm^{-1} band in MA splits into two bands in TFM that appear at 390 and 324 cm^{-1} . This splitting arises from coupling between out of plane ring deformation and C–CHO out of plane bending mode. The C–CHO out of plane bending mode is also correlated to one of the out of plane ring deformation modes, which are calculated at 131 cm^{-1} .

Theoretically, the symmetric hydrogen bond stretching for MA and TFM are expected to be observed at 265 and 278 cm^{-1} , respectively. This upward frequency shift by formyl substitution in α -position also supports the stronger hydrogen band in TFM compared with that in MA. Similar relation between the $\text{O}\cdots\text{O}$ stretching frequency and hydrogen bond strength are observed in the substituted acetyl acetone: Hexafluoro-AA < acetyl acetone < α -Cyano-AA.

Theoretical frequencies for these compounds are 238 [45], 372 [14] and 387 cm^{-1} [46], respectively.

5.5. Conclusion

According to all used ab initio calculation, except for B3LYP/STO-3G, The *trans* conformer is more stable than the *cis* conformer. The energy difference depends to the choice of level and increases by increasing the size of the basis sets.

Similarly, the present calculations show a π -electron delocalization through $\text{O}_{10}=\text{C}_9-\text{C}_3=\text{C}_4-\text{O}_5$ fragment of the molecule and reduced electron delocalization in $\text{O}_1=\text{C}_2-\text{C}_3$ fragment of the chelated ring. Furthermore, geometrical analysis indicates that formyl substitution in α -position increases the hydrogen bond strength, which is in agreement with the $^1\text{H-NMR}$ and IR results. According to the theoretical calculations, at B3LYP/6-311++G** level, the IHB stabilized the *cis* enol form of TFM by 56 kJ mol^{-1} .

Comparison of theoretical and experimental rotational constants and vibrational frequencies indicates that the B3LYP/6-311++G** level gives the best results among all other used DFT levels, but the results of B3LYP/6-31G** are also reliable.

References

- [1] A.H. Lowery, C. George, P.D. Antonio, J. Karle, J. Am. Chem. Soc. 93 (1971) 6399.
- [2] R.S. Brown, A.T. Nakashima, R.C. Haddon, J. Am. Chem. Soc. 101 (1979) 3175.
- [3] J. Emsley, Structure and Bonding, vol. 2, Springer, Berlin, 1984.
- [4] R. Boese, M.Y. Antipin, D. Blaser, K.A. Lyssenko, D. Bläser, K.A. Lyssenko, J. Phys. Chem. B 102 (1998) 8654.
- [5] W.O. George, V.G. Mansell, J. Chem. Soc. B (1968) 132.
- [6] R.S. Noi, B.A. Ershov, A.I. Koltsov, Z. Org. Khim. 11 (1975) 1778.
- [7] R. Boese, M.Y. Antipin, D. Blaser, K.A. Lyssenko, J. Phys. Chem. B 102 (1998) 8654.
- [8] K. Iijima, A. Ohnogi, S. Shibata, J. Mol. Struct. 156 (1987) 111.
- [9] A. Camerman, D. Masteropalo, N. Camerman, J. Am. Chem. Soc. 105 (1983) 1584.
- [10] M.A. Rios, J. Rodriguez, J. Mol. Struct. (Theochem) 204 (1990) 137.
- [11] F. Hibbert, J. Emsley, Hydrogen Bonding and Chemical Reactivity. Advance in Physical Chemistry, vol. 26, Academic Press, London, 1990, p. 255.
- [12] S.F. Tayyari, F. Milani-Nejad, Spectrochim. Acta A 54 (1998) 255.
- [13] S.F. Tayyari, T. Zeegers-Huyskens, J.L. Wood, Spectrochim. Acta A 35 (1979) 1289.
- [14] S.F. Tayyari, F. Milani-Nejad, Spectrochim. Acta A 56 (2000) 2681.
- [15] S.F. Tayyari, Ph.D. Thesis, London University, 1978.
- [16] S.F. Tayyari, T. Zeegers-Huyskens, J.L. Wood, Spectrochim. Acta A 35 (1979) 1265.
- [17] T. Chiavassa, P. Verlaque, L. Pizalla, P. Roubin, Spectrochim. Acta A 50 (1993) 343.
- [18] T. Chiavassa, P. Roubin, L. Pizalla, P. Verlaque, A. Allouche, F. Marinelli, J. Phys. Chem. 96 (1992) 659.
- [19] H. Ogoshi, K. Nakamoto, J. Chem. Phys. 45 (1966) 3113.
- [20] C. Nonhebel, Tetrahedron 24 (1968) 1896.
- [21] J. Emsley, L.Y.Y. Ma, S.C. Nyburg, A.W. Parkins, J. Mol. Struct. 240 (1990) 59.
- [22] J. Emsley, L.Y.Y. Ma, M. Motevalli, J. Chem. Soc. Perkin Trans. 2 (1989) 527.
- [23] J. Emsley, L.Y.Y. Ma, M. Motevalli, M.B. Hursthouse, J. Mol. Struct. 216 (1990) 143.
- [24] J. Emsley, N.J. Freeman, P.A. Bates, J. Chem. Soc. Perkin Trans. 1 (1988) 297.
- [25] G. Buemi, F. Zuccarello, Electr. J. Theor. Chem. 2 (1997) 302.
- [26] N.D. Sanders, Ph.D. Thesis, Harvard University, 1979.
- [27] W. Caminati, personal communication.
- [28] Z. Arnold, J. Zemlicka, Coll. Czech. Chem. Commun. 25 (1960) 1318.
- [29] L.W. Reeves, Can. J. Chem. 35 (1957) 1351.
- [30] K.M. Keshavarz, K.M. Cox, R.O. Angus, Synthesis 8 (1988) 641.
- [31] P.H. Turner, J. Chem. Soc. Faraday Trans. 2 76 (1980) 383.
- [32] M. Budesinsky, P. Feidler, Z. Arnold, Synthesis 11 (1988) 746.
- [33] M.J. Frisch, G.W. Trucks, H.B. Schlegel, F.E. Scuseria, M.A. Robb, J.R. Cheeseman, V.G. Zakrzewski, J.A.G. Montgomery, R.E. Stratmann, J.C. Burant, S. Dapprich, J.M. Millam, A.D. Daniels, K.N. Kudin, M.C. Strain, O. Farkas, J. Tomasi, V. Barone, M. Cossi, R. Cammi, B. Mennucci, C. Pomelli, C. Adamo, S. Clifford, J. Ochterski, G.A. Petersson, P.Y. Ayala, Q. Cui, K. Morokuma, D.K. Malick, A.D. Rabuck, K. Raghavachari, J.B. Foresman, J. Cioslowski, J.V. Ortiz, B.B. Stefanov, G. Liu, A. Liashenko, P. Piskorz, I. Komaromi, R. Gomperts, R.L. Martin, D.J. Fox, T. Keith, M.A. Al-Laham, C.Y. Peng, A. Nanayakkara, C. Gonzalez, M. Challacombe, P.M.W. Gill, B. Johnson, W. Chen, M.W. Wong, J.L. Andres, C. Gonzalez, M. Head-Gordon, E.S. Replogle, J.A. Pople, GAUSSIAN 98, Revision A.3, Gaussian, Inc, Pittsburgh, PA, 1998.
- [34] A.D. Becke, Phys. Rev. A 38 (1988) 3098.
- [35] A.D. Becke, J. Chem. Phys. 98 (1993) 5648.

- [36] P.M.W. Gill, *Mol. Phys.* 89 (1996) 433.
- [37] J.P. Perdew, Y. Wang, *Phys. Rev. B* 45 (1992) 1324.
- [38] C. Lee, W. Yang, R.G. Parr, *Phys. Rev. B* 37 (1988) 875.
- [39] G. Buemi, F. Zuccarello, *Electr. J. Theor. Chem.* 2 (1997) 118.
- [40] Z. Smith, E.B. Wilson, R.W. Durest, *Spectrochim. Acta A* 39 (1983) 117.
- [41] V. Bertolasi, P. Gilli, V. Ferretti, G. Gilli, *J. Am. Chem. Soc.* 113 (1991) 4917.
- [42] A.A. Bothner, R.K. Harris, *J. Org. Chem.* 30 (1965) 254.
- [43] N.N. Shapetko, A.V. Kessenikh, A.P. Skoldinov, A.P. Protopopva, *Teor. Eksper. Khim.* 2 (1966) 757.
- [44] N.B. Colthup, L.H. Daly, S.E. Wiberly, *Introduction to Infrared and Raman Spectroscopy*, second ed, 1975.
- [45] S.F. Tayyari, F. Milani-Nejad, H. Rahemi, *Spectrochim. Acta, A* 58 (2002) 1669.
- [46] S.F. Tayyari, H. Raissi, F. Milani-Nejad, I.S. Butler, *Vibration. Spectrosc.* 814 (2001) 1.